



Technical Note

Analysis of the ideal gas flow over body of basic geometrical shape

Sergei V. Ryzhkov^{a,*}, Victor V. Kuzenov^{a,b}^a Bauman Moscow State Technical University, 2-nd Bauman Street, 5, 1, Moscow 105005, Russian Federation^b Dukhov Research Institute of Automatics (VNIIA), Sushchevskaya Str. 22, Moscow 127055, Russian Federation

ARTICLE INFO

Article history:

Received 22 June 2018

Received in revised form 4 December 2018

Accepted 5 December 2018

Keywords:

Gas dynamics

Boundary layer

Mathematical model

Shock wave

ABSTRACT

An approximate mathematical model of the heat transfer processes in the laminar and turbulent boundary layers, which occur near the surface of an aircraft moving at the hypersonic speed in the Earth's atmosphere, is derived. This mathematical model makes it possible to calculate the convective heat transfer on the surface of typical structural elements of modern perspective aircrafts. 2D versions of the calculations of convective heat fluxes for bodies of simple geometric shapes are performed.

© 2018 Elsevier Ltd. All rights reserved.

1. Introduction

The study of the gas dynamics of the high-velocity ($M > 6$) flow around bodies with simple geometric shapes is determined by the fact that, firstly, these structural elements are the key elements of aircrafts, and secondly, the known construction materials used to manufacture typical elements (basic geometric bodies) of modern aircrafts at the speeds of $M \sim 6$ reach the limit of their thermo-strength capabilities.

We also note that many physical problems arise when designing the advanced aircrafts, e.g. the effect of the friction coefficient on the motion with the hypersonic speed, and also the determination of viscous tangential stresses on the streamlined surface of a body under various flow regimes; the effect of the convective flow on the thermophysical characteristics of the flow around the body, and the determination of the external thermal loads on the construction of an aircraft.

Both problems are associated with the appearance of thermal and dynamic boundary layers on the outer surface of an aircraft moving in a continuous medium. Moreover, in the case of a vehicle moving with the high speed ($M > 6$), the velocity gradients across the boundary layer (and also the frictional forces) increase appreciably if they are compared with the case of an aircraft with the supersonic speed. In a narrow (in comparison with the characteristic size of a streamlined body) hypersonic boundary layer, the work of friction forces leads to the intense energy release, i.e. the boundary layer can be considered as a narrow spatial region adjacent to

the surface of the streamlined body, in which there is an intense heat release due to the energy dissipation processes. These dissipation processes are accompanied by the strong change in the thermophysical (density, pressure, temperature, viscosity, thermal conductivity, etc.) and dynamic properties of the gas, as well as heat flows directed to the surface of the aircraft. These processes, in turn, should be analyzed analytically and numerically.

The approach in the computational hydro- and gas dynamics based on the numerical integration of the complete system of Navier-Stokes equations is the most promising for studying these processes. However, the solution of such problems, as a rule, requires large computer time costs (a very detailed computational grid is required in the boundary layer because its thickness is about 1 mm). The results of calculations can depend strongly on the structure of the computational grid, the size of the calculated area, the input parameters, and the features of the calculation algorithm. In view of the above reasons, the use of the Navier-Stokes equations for the rapid evaluation of heat fluxes is quite problematic. Therefore, in this physically complicated case, an analogy with the body of the simplest form, e.g. a plate or a cone, is used to estimate the heat fluxes on the surface of a simple-shape body. At the same time, the geometric parameters of simple-shape bodies are selected for each section of such a surface, the regularities of the development of the boundary layer on which are known [1–8]. To determine the heat flux in this way, it is necessary to know the distribution of the gas-dynamic parameters at the outer boundary of the boundary layer (by solving the Euler equations). We note that this approach is applicable only where the thin boundary layer model works. In the tear-off zones, this method

* Corresponding author.

E-mail address: svryzhkov@bmstu.ru (S.V. Ryzhkov).

can give a qualitatively incorrect result, because the flow separation has a viscous nature [4–8].

In this case, the experimental studies are very expensive. At the same time, in terrestrial conditions, the simulation of the physico-chemical processes accompanying the flights of prospective aircraft in the Earth's atmosphere is technically difficult. For this reason, it is necessary to determine the aerodynamic characteristics by calculations and theoretical methods.

2. Numerical simulation of convective heat fluxes near bodies of simple geometric shapes

The mathematical model of the thermophysical processes, which arise when bodies with simple geometric shapes are streamlined, is based on the equations of gas dynamics (the height range from the Earth's surface, where the calculation are to be performed, is $H = 25 \div 40$ km). The coordinate transformation of the form $r = r(\xi, \eta, \zeta)$, $z = z(\xi, \eta, \zeta)$, $\varphi = \varphi(\xi, \eta, \zeta)$ is introduced using the finite-difference method in order to solve the system of equations of gas dynamics. In dimensionless variables, this system of equations takes the following form [2]:

$$\frac{\partial \rho}{\partial t} + \text{Div}(\rho \vec{V}) = -\alpha \frac{\rho u}{r},$$

$$\begin{aligned} \frac{\partial \rho u}{\partial t} + \text{Div}(\rho u \vec{V}) &= -\xi_r \frac{\partial P}{\partial \xi} - \eta_r \frac{\partial P}{\partial \eta} - \alpha \frac{\rho u^2}{r} + \frac{\partial \rho v}{\partial t} + \text{Div}(\rho v \vec{V}) \\ &= -\xi_z \frac{\partial P}{\partial \xi} - \eta_z \frac{\partial P}{\partial \eta} - \alpha \frac{\rho u v}{r}, \end{aligned}$$

$$\frac{\partial \rho e}{\partial t} + \text{Div}(\rho e \vec{V} + \sum \vec{q}_i) = -\frac{P}{J} \text{Div}(\vec{V}) - \alpha \frac{P u}{r} - \alpha \frac{\rho e u}{r},$$

$$S_e = \mu_\Sigma D + \frac{\gamma}{Pr} \text{div}(\lambda_\Sigma \text{grad} T),$$

where $u(r, z, t), v(r, z, t)$ are projections of the velocity vector $\vec{V}(r, z, t)$ on R and Z axes, e is the specific internal plasma energy, $J = \partial(r, z) / \partial(\xi, \eta)$ is the Jacobian transition the cylindrical coordinate system r, z to the curvilinear coordinates ξ, η , $V_\xi = \xi_r u + \xi_z v$, $V_\eta = \eta_r u + \eta_z v$ are the contravariant components of the velocity vector \vec{V} in the curvilinear coordinates ξ, η , ρ, P are the plasma density and pressure, respectively, $\alpha = 0$ corresponds to the plane flow, and $\alpha = 1$ corresponds to axisymmetric flow.

The computational region included the flow field in the undisturbed flow, those behind the front of the shock wave and in the wake of the streamlined body, and it was a curvilinear rectangle in the coordinate system r, z (it was a rectangle in the coordinate system ξ, η).

In the lower part of the rectangle, either the axis of symmetry or the solid surface is perpendicular to the surface. From the top, it was bounded by a straight line on which the "non-perturbing" conditions are set on the flow leaving the computational region:

$\partial^2 \vec{f} / \partial x_n^2 = 0$ where $\vec{f} = \{\rho, u, v, e\}$ and x_n is the coordinate normal to the boundary surface. On the right-hand side, the integration region is limited by a straight line, on which the parameters of the air flow incoming onto the body with simple geometric shape are specified. On the left-hand side, a surface is located, which is sufficiently far from the right-hand boundary and corresponds to the conditions at infinity.

The numerical method used for the calculation is based on the nonlinear quasi-monotonic compact-polynomial difference scheme of high-order accuracy and spatial splitting of the Euler equations [9] written in the arbitrary curvilinear coordinate system. The procedure for calculating the breakdown of a discontinuity developed by S.K. Godunov, Full member of the Russian

Academy of Sciences, was used to determine the mass and energy flux vectors at the boundaries of the computational cell. The computational grid (and the adapted curvilinear coordinate system) was created using the technique described in [10–11]. The applied computational codes use the multi-block calculation technology on non-orthogonal structured grids.

We note that the calculation of heat fluxes in the considered case is always preceded by the determination of the external inviscid flow near the surface of the streamlined body. The method of calculating the heat flux, which occurs on the surface of bodies with simple geometric shapes, is described in Refs. [4–7, 12–15, 18–20].

In the laminar case, the heat flux near the critical point can be estimated using the formula [16–20]:

$$q_w = 1,93 \times 10^{-4} V_\infty^{1,08} (H_0 - H_w) \sqrt{\frac{\rho_\infty}{R}}.$$

In the turbulent case, it can be estimated using the formula [16, 17]:

$$q_w = 4,69 \times 10^{-4} V_\infty^{1,25} (H_0 - H_w) \left(1 + \frac{T_w}{T_0}\right)^{-\frac{2}{3}} \frac{\rho_\infty^{0,8}}{R^{0,2}},$$

where $H_w, J/kg, T_w, K$ are the enthalpy and temperature on the surface of a streamlined body, respectively, $H_0, J/kg, T_0, K$ are the enthalpy and temperature, respectively, taken on the outer boundary of the boundary layer, $\rho_\infty, kg/m^3, V_\infty, m/s$ are the density and velocity of the undisturbed flow incoming onto the body, $R, m, q_w, W/m^2$ are the radius of curvature of the body, and heat flux at the front critical point, respectively.

It follows from the above formulas that the heat transfer coefficient in the critical point is inversely proportional to the square root \sqrt{R} (in the turbulent case, it is proportional to $R^{0,2}$) of the blunting radius R . Therefore, at high flight speeds and, correspondingly, large deceleration temperatures, the values of the convective and radiative fluxes increase sharply in the critical point when the blunting radius decreases. We consider the application of the effective length method in the point with the Cartesian coordinate x_* for the case of the rotation body with the radius $R(x_*)$. Here l_* is the length of the arc formed from the beginning of the body to the considered point. We assume that a thermal boundary layer with the thickness δ is formed on the body at the point (x_*, R) . The effective length x_{eff} is the length of a flat plate, on which the same boundary layer grows as on the length of considered body, when the external flow has the same parameters as that at the considered point of the body. For an axially symmetrical case, the effective length x_{eff} is the length of a cylinder with the radius R .

To reduce to a dimensionless form, we introduce the following notation for dimensionless variables:

$$\bar{R} = \frac{R}{R_*}, \bar{\mu} = \frac{\mu_0}{\mu_\infty}, \bar{\rho} = \frac{\rho_0}{\rho_\infty}, \bar{\mu}_w = \frac{\mu_w}{\mu_\infty}, \bar{\rho}_w = \frac{\rho_w}{\rho_\infty},$$

$$\bar{U} = \frac{U_0}{U_\infty}, \bar{T}_w = \frac{T_w}{T_\infty}, \bar{T}_e = \frac{T_e}{T_\infty}, \bar{T}_r = \frac{T_r}{T_\infty}, \bar{T}_0 = \frac{T_0}{T_\infty},$$

$$\bar{C}_p = \frac{C_{p,0}}{C_{p,\infty}}, \bar{q}_w = \frac{q_w}{\rho_\infty U_\infty (C_p)_{cp}^* T_\infty},$$

where R_* is the body curvature radius at flow deceleration point, $\mu_\infty, \rho_\infty, U_\infty, T_\infty, C_{p,\infty}$ are the viscosity, density, velocity, temperature and heat capacity at $p = \text{const}$ in the flow of body, $\mu_0, \rho_0, U_0, C_{p,0}$ are the viscosity, density, velocity, and heat capacity taken at the outer boundary of the boundary layer in the considered cross-section with the Cartesian coordinate x along the streamlined body, μ_w, ρ_w are the viscosity and density at wall temperature, T_w, T_e are the surface temperature of the streamlined body and the

temperature of the heat-insulated wall, T_r is the ambient recovery temperature, $\bar{T}_r = \bar{T}_0 \left(1 + r \frac{\gamma-1}{2} M_0^2\right)$.

The effective length method is used in Ref. [17] to calculate the heat exchange of bodies with classical shapes (plate, cylinder, cone, sphere, etc.) with the gas flow, in which the main parameters vary along their lengths. According to this method (for the laminar flow), the effective length x_{eff} is determined by the relation [14–17]:

$$x_{eff} = \frac{\int_0^x \left[\bar{R}^2 K^2 K_1^2 \bar{\mu} \bar{U} \bar{C}_{p,0}^2 (\bar{T}_e - \bar{T}_w)^2 Pr_0^{-\frac{4}{3}} \right] dx}{\left[\bar{R}^2 K^2 K_1^2 \bar{\mu} \bar{U} \bar{C}_{p,0}^2 (\bar{T}_e - \bar{T}_w)^2 Pr_0^{-\frac{4}{3}} \right]}$$

The quantities varying from the beginning of the formation of the boundary layer (the critical point) to the considered cross-section using the Cartesian coordinate x are under the integral. $R(x)$ is the rotation radius of the axisymmetric body, M_0, Pr_0 are the local Mach and Prandtl numbers taken at the outer boundary of the boundary layer in the considered cross-section with the Cartesian coordinate $x, r = \sqrt{Pr_0}$, where r is the temperature recovery factor (it shows what fraction of the kinetic energy of the external flow goes to increase the heat content of the gas near the surface of the streamlined body).

For accelerated and slowly retarded flows, the coefficient K_1 in the expression for the effective length x_{eff} . It takes into account the effect of the longitudinal velocity gradient. This parameter is close to unity and mainly depends on the velocity gradient parameter and the temperature factor: $K_1 = \left[1 + 0,16 \left(1 + \frac{\bar{T}_w}{\bar{T}_0} \right) \left(\frac{2m}{m+1} \right)^{1/3} \right]^{1/2}$.

The coefficient K is a factor, which accounts for the effect of the compressibility: $K = \left(\frac{\bar{\mu}}{\rho_w \mu_w} \right)^{1/3}$. The value of the dimensionless velocity gradient m follows from the formula: $m = \frac{x}{V_0} \frac{\partial V_0}{\partial x}$. The determining temperature T^* has the form:

$$\bar{T}_0^* = 1 + 0,5 \cdot (\bar{T}_w - 1) + 0,22 \cdot (\bar{T}_r - 1), \quad \bar{T}_r = \bar{T}_0 + r \frac{\bar{U}_0^2}{\left[2(C_p)_{cp}^* T_\infty / U_\infty^2 \right]}$$

$r = \sqrt{Pr_0}$, where $(C_p)_{cp}^*$ is the average value of the heat capacitance, determined in the temperature range $[T, T^*]$.

The value of the Stanton number can be found using the relation:

$$St_{x,eff} = 0,332(m+1)^{1/2} Re_{x,eff}^{1/2} Pr_0^{-2/3} K \cdot K_1.$$

In this relation, the Reynolds number is determined by the following formula:

$$Re_{x,eff} = \frac{\rho_w V_0 x_{eff}}{\mu_w}$$

where ρ_w, μ_w are taken from the surface temperature of the body T_w .

The heat convective flux q_w in the laminar case follows from the relation:

$$\bar{q}_w = \bar{\rho} \bar{V} (\bar{T}_e - \bar{T}_w) St_{x,eff}.$$

In the turbulent flow regime near the surface of the streamlined body, the following formula for calculating the effective length x_{eff} can be used [16,17,19]:

$$x_{eff} = \frac{\int_0^x \left[\bar{R}^{5/4} \left(1 + r \frac{\gamma-1}{2} M_0^2 \right)^{0,1375} \bar{\rho} \bar{U} Pr_0^{-0,7125} \bar{\mu}^{0,25} \bar{C}_{p,0}^{1,25} \right] (\bar{T}_w / \bar{T}_e)^{0,5} (\bar{T}_e - \bar{T}_w)^{1,25} dx}{\left[\bar{R}^{5/4} \left(1 + r \frac{\gamma-1}{2} M_0^2 \right)^{0,1375} \bar{\rho} \bar{U} Pr_0^{-0,7125} \bar{\mu}^{0,25} \bar{C}_{p,0}^{1,25} \right] (\bar{T}_w / \bar{T}_e)^{0,5} (\bar{T}_e - \bar{T}_w)^{1,25}}$$

where the temperature recovery factor is $r = \sqrt[3]{Pr_0}$, and the value of the heat flux is given by:

$$\bar{q}_w = \bar{\rho} \bar{V} (\bar{T}_e - \bar{T}_w) St_{x,eff}, \quad Re_{x,eff} = \frac{\rho_w V_0 x_{eff}}{\mu_w}.$$

The value of the Stanton number for the turbulent regime can be found using the relation:

$$St_{x,eff} = 0,0296 Re_{x,eff}^{-0,2} Pr_0^{-0,57} (\bar{T}_w / \bar{T}_e)^{0,4} \left(1 + r \frac{\gamma-1}{2} M_0^2 \right)^{0,11}.$$

Using the assumptions of [19], the Stanton number $St_{x,eff}$ for the transition region of the flow can be determined from the formula:

$$St_{x,eff} = St_{x,eff,turb} - (St_{x,eff,turb} - St_{x,eff,lam}) \exp \left[\frac{Re_{x,eff} - Re_{x,eff,n}}{Re_{x,eff,n}} \right],$$

where $St_{x,eff,turb}, St_{x,eff,lam}$ are determined by the formulas given above in the text; $Re_{x,eff,n}$ is the Reynolds number for the onset of the transition from the laminar to the turbulent flow. This dependence is in good agreement with the experimental data [19–23] for the flow conditions $Re_{x,eff} = 10^4 \div 10^6$.

3. Calculation results

The calculation of the flow around blunted axisymmetric bodies is used for the validation and verification of this mathematical model of the heat transfer near the surface of the characteristic elements of an aircraft (in this case, the calculated and experimental data from [23] can be used).

The computational region includes the flow field in the undisturbed flow and those behind the front of the shock wave and in the wake of the streamlined body. The initial data for the calculations performed in the work are shown in Tables 1 and 2 (see Table 3).

These calculations are performed for Mach numbers of $M = 6-10$ and flight heights of $h = 22$ km and $h = 37$ km in the Earth's atmosphere.

The calculation results of the density of the convective heat flux q_w according to the one-temperature model of the dissociation kinetics [23] are shown in Fig. 1a (the height of $h = 22$ km), and Fig. 1b shows the densities of the convective heat flux q_w obtained by the developed method.

The initial data for the calculations performed in Ref. [15] are indicated in Table 1 and Table 2. These calculations were performed for Mach numbers $M = 6-10$ and altitudes $h = 22$ km and $h = 37$ km in the Earth's atmosphere.

Table 1
Parameters of the air atmosphere.

Parameter	Value	Value	Dimension
Flight Height	22	37	km
Downstream pressure	0.405 10 ⁵	0.433 10 ⁴	erg/cm ³ (Tor)
The temperature of the oncoming stream	219	242	K
Density	0.645 10 ⁻⁴	0.624 10 ⁻⁵	g/cm ³
Sound speed	0.296 10 ⁵	0.312 10 ⁵	cm/s
Frequency of collisions	0.317 10 ⁹	0.323 10 ⁸	1/s
The mean free path	0.126 10 ⁻³	0.13 10 ⁻²	cm

Table 2
Initial data for calculations of flow around a spherically blunted cylinder.

Parameter	Case 1	Case 2	Dimension
P_∞	0.23 10 ⁴	0.23 10 ⁵	erg/cm ³ (Tor)
ρ_∞	0.178 10 ⁻⁵	0.433 10 ⁻⁴	g/cm ³
V_∞	4.167 10 ⁵	4.167 10 ⁵	cm/c
T_∞	450	450	K

Table 3
Parameters of the flow.

Pressure in the flowing stream	$P = 1120$ Pa
Speed in the incoming flow	$V = 945$ m/s
Temperature in the flowing stream	$T = 62.1$ K
Mach number in the flowing stream	$M = 6$
Composition that flows into the body of the gas	Air
Height from the surface of the Earth	$H = 25$ km

Fig. 1a (height $h = 22$ km) shows the results of calculating the convective heat flux q_w density from a single-temperature dissociation kinetics model [23], and Fig. 1b shows the convective heat flux q_w density by a method developed by the authors.

The convective heat flux density distributions q_w along the streamlined non-catalytic surface of a cylinder blunted on the sphere are shown in Fig. 3 (variant 1). Here in Fig. 3, the dotted curves correspond to the results given in [23], and the solid lines

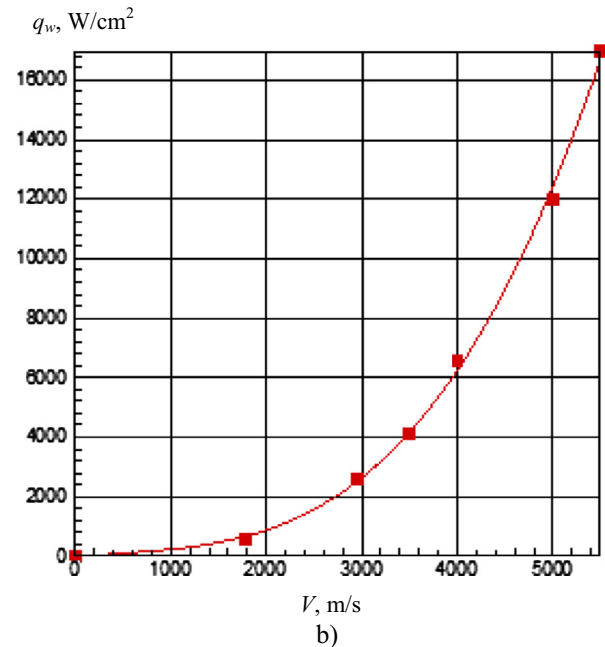
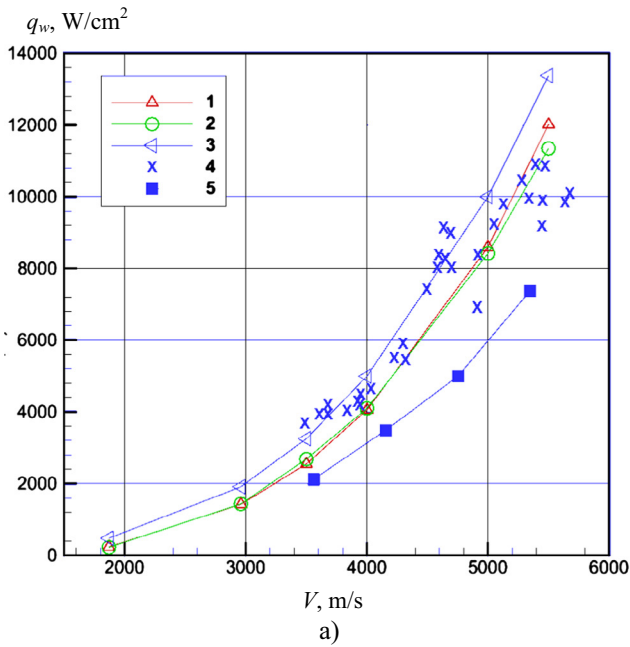


Fig. 1. Density of convective heat fluxes at the critical point blunted over the sphere of the cylinder (radius of blunting $R = 0.66$ cm) at zero angle of attack for flight altitude $h = 22$ km. (a) The results given in [23]. (b) The results obtained in this paper.

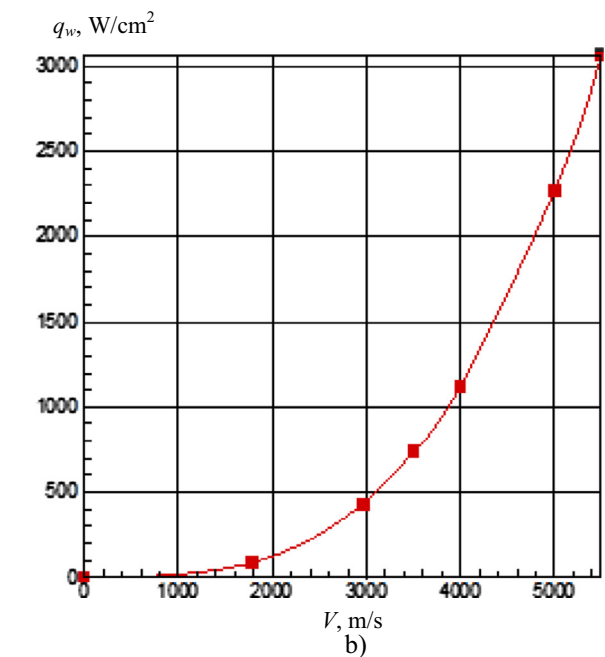
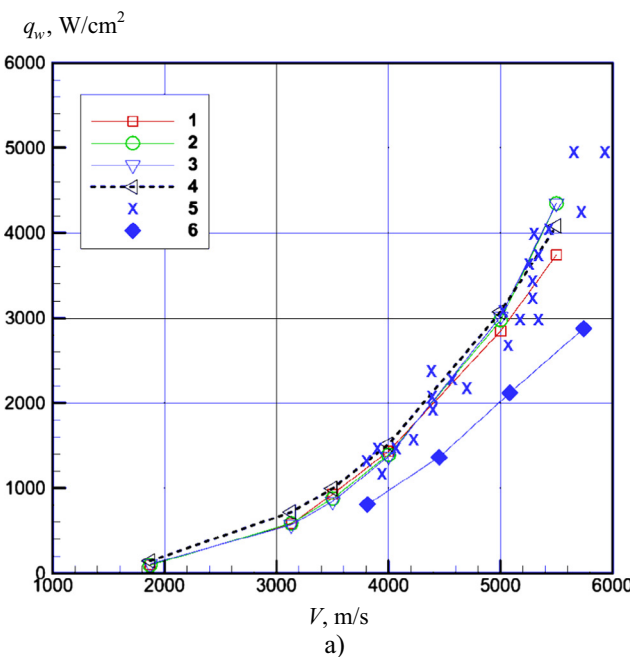


Fig. 2. Convective heat flux density at the critical point of a cylinder blunted on the sphere (the blunting radius of $R = 0.66$ cm) at the zero angle of attack for the flight height of $h = 37$ km. (a) Results given in [23]. (b) Results obtained in this work.

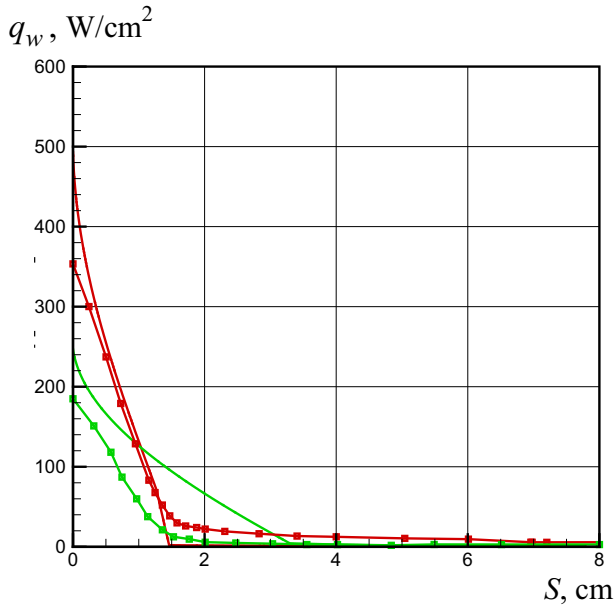


Fig. 3. Convective heat flux density distribution along the surface of a cylinder blunted on the sphere. Blunting radii are $R = 1.27$ cm and $R = 5.08$ cm (variant 1). Non-catalytic surface ($M = 9.8$).

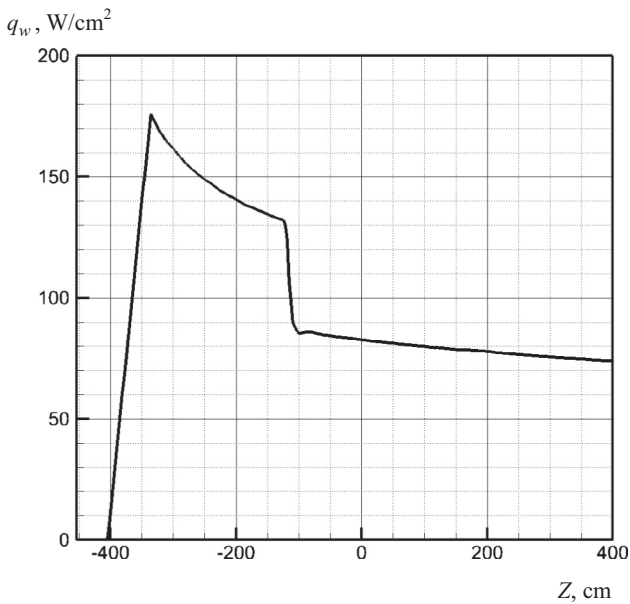


Fig. 4. Convective heat flux dependence on the longitudinal coordinate (the wedge conjugated to the wedge).

are obtained by the developed approximate engineering method for calculating the convective heat transfer.

Fig. 2 (the height of $h = 37$ km) shows the densities of convective heat fluxes at the critical point of a cylinder blunted around the sphere for the thermal equilibrium conditions, as well as for the conditions of accounting for the effect of the vibrational relaxation on dissociation (Fig. 2a [23]) and the results of this work are shown in Fig. 2b. According to the graphical dependences (Figs. 1 and 2), the following estimate of the error in calculating the convective heat flux q_w is possible: 37% – $h = 22$ km and 22% – $h = 37$ km.

It follows from the graphical dependences (Fig. 3) that for the blunting radius $R = 1.27$ cm (red curve) the convective heat flux

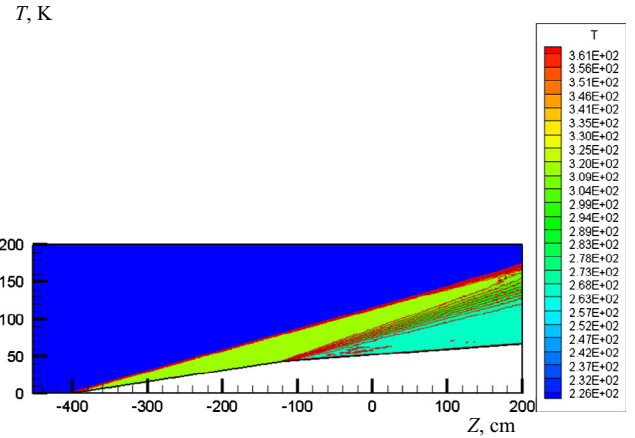


Fig. 5. Temperature distribution at the flow around a sharp wedge.

density distribution q_w along the surface of a cylinder blunted on the sphere on average has the error $\leq 20\%$. More noticeable discrepancies in the calculations of the convective heat flux density q_w given in Fig. 3 (green curve) are observed for the blunting radius of $R = 5.08$ cm.

The results of calculations show that the errors in the deviation of the inclination angle β of the shock wave are $\leq 1\%$, and those in the gas-dynamic quantities are on the order of 3%. The calculation is performed for the cone (the opening angle of the cone is 9 degrees) conjugated to the cone (the opening angle of the cone is 4 degrees). The following parameters of the incoming air flow were used for the calculation of the heat transfer near the surface of bodies of simple geometric shapes:

Some results of calculations of the vector and scalar fields of aerothermodynamic parameters using the above mathematical model of the heat transfer near the surface of the characteristic elements of the aircraft are shown in Figs. 4 and 5: the wedge (the opening angle of the wedge of 9 degrees) conjugated to the wedge (the opening angle of the wedge of 4 degrees).

It follows from the graphical dependences (Figs. 4 and 5) that the flow structure near the wedge conjugated to the wedge consists of a stationary plane shock wave attached to the “sharp” part of the wedge (with the gas dynamic parameters: $T = 314$ K, $P = 0.065$ atm, $\rho = 7.06 \cdot 10^{-5}$ kg/m³) and plane rarefaction wave (directly behind: $T = 267$ K, $P = 0.037$ atm, $\rho = 4.8 \cdot 10^{-5}$ kg/m³) arising in the kink point of the streamlined body.

The maximal intensity of the convective heating predicted by calculations (Fig. 4) is near the front critical point and its level is approximately $q_w = 170$ kW/m². We also note that a sharp (by 40%) drop in the convective heat flow q_w (due to the cooling of the gas flow) is observed behind the rarefaction wave.

4. Conclusion

This work presents a mathematical model derived for a fast initial estimate of aerothermodynamics of typical key elements of perspective aircrafts in the region of laminar and turbulent boundary layers (in the speed and height ranges of $M = 6-10$ and $H = 22-37$ km, respectively). This model is verified and validated (the accuracy of the results obtained using the approximate model is close to that of the results obtained using much more complete computational models) and includes the calculation of gas-dynamic parameters (based on the Euler equations), and also the approximate calculation of the convective heat flux near the surface of simple-shape bodies.

Conflict of interest

The authors declared that there is no conflict of interest.

Acknowledgments

This work was supported by the Ministry of Science and Higher Education of the Russian Federation, Project No 13.5240.2017/8.9.

References

- [1] N.N. Smirnov, V.B. Betelin, R.M. Shagaliev, V.F. Nikitin, I.M. Belyakov, Yu.N. Deryuguin, S.V. Aksenov, D.A. Korchazhkin, Hydrogen fuel rocket engines simulation using LOGOS code, *Int. J. Hydrogen Energy* 39 (2014) 10748–10756.
- [2] F. Chen, H. Liu, S. Zhang, Coupled heat transfer and thermo-mechanical behavior of hypersonic cylindrical leading edges, *Int. J. Heat Mass Transf.* 122 (2018) 846–862.
- [3] S.T. Surzhikov, Convective heating of small-radius spherical blunting for relatively low hypersonic velocities, *High Temp.* 51 (2013) 231–245.
- [4] M.E. Tauber, K. Sutton, Stagnation-point radiative heating relations for earth and Mars entries, *J. Spacecraft* 28 (1991) 40–42.
- [5] E.V. Zoby, J.N. Moss, K. Sutton, Approximate convective heating analysis for hypersonic flows, *J. Spacec. Rock.* 18 (1981) 64–70.
- [6] H.H. Hamilton, K.J. Weilmuenster, F.R. DeJanette, Improved approximate method for computing convective heating on hypersonic vehicles using unstructured grids, *AIAA* (2006) 2006–3394.
- [7] F.R. DeJanette, H.H. Hamilton, K.J. Weilmuenster, New method for computing convective heating in stagnation region of hypersonic vehicles, *AIAA* 2008 (2008).
- [8] S.T. Surzhikov, Computing system for solving radiative gasdynamic problems of entry and re-entry space vehicles, in: 1st International Workshop on Radiation of High Temperature Gases in Atmospheric Entry ESA-533, 2003, pp. 111–118.
- [9] V.V. Kuzenov, S.V. Ryzhkov, Numerical modeling of laser target compression in an external magnetic field, *Math. Models Comput. Simul.* 10 (2018) 255–264.
- [10] V.V. Kuzenov, A.O. Dobrynina, V.V. Shumaev, Calculating processes of laminar and turbulent heat transfer around the elements of the aircraft, *J. Phys. Conf. Ser.* 980 (2018) 012023.
- [11] V.V. Kuzenov, S.V. Ryzhkov, Numerical simulation of the effect of laser radiation on matter in an external magnetic field, *J. Phys. Conf. Ser.* 830 (2017) 012124.
- [12] E. Josyula, J. Shang, Computation of nonequilibrium hypersonic flow- fields around hemisphere cylinders, *J. Thermophys. Heat Transf.* 7 (1993) 668–679.
- [13] S. Ju, C. Yan, X. Wang, Y. Qin, Z. Ye, Sensitivity analysis of geometric parameters upon the aerothermodynamic performances of Mars entry vehicle, *Int. J. Heat Mass Transf.* 120 (2018) 597–607.
- [14] V.V. Shumaev, V.V. Kuzenov, Development of the numerical model for evaluating the temperature field and thermal stresses in structural elements of aircrafts, *J. Phys. Conf. Ser.* 891 (2017) 012311.
- [15] V.V. Kuzenov, S.V. Ryzhkov, Approximate method for calculating convective heat flux on the surface of bodies of simple geometric shapes, *J. Phys. Conf. Ser.* 815 (2017) 012024.
- [16] V.V. Lunev, *Real Gas Flows with High Velocities*, CRC Press, 2010.
- [17] V.V. Znamenskii, V.V. Lunev, Asymptotic properties of the equations of the film theory of ablation in problems when the shape of the bodies changes as a result of aerodynamic heating, *Fluid Dyn.* 16 (1981) 34.
- [18] N.N. Smirnov, V.B. Betelin, V.F. Nikitin, L.I. Stamov, D.I. Altoukhov, Accumulation of errors in numerical simulations of chemically reacting gas dynamics, *Acta Astronautica* 117 (2015) 338–355.
- [19] C. Liu, W. Cao, Study of predicting aerodynamic heating for hypersonic boundary layer flow over a flat plate, *Int. J. Heat Mass Transf.* 111 (2017) 1079–1086.
- [20] B. Shotorban, G.B. Jacobs, O. Ortiz, Q. Truong, An Eulerian model for particles nonisothermally carried by a compressible fluid, *Int. J. Heat Mass Transf.* 65 (2017) 845–854.
- [21] G.N. Abramovich, *Applied Gas Dynamics*, Nauka, Moscow, 1976 (in Russian).
- [22] N.Y. Fabrikant, *Aerodynamics. General Course*, Nauka, Moscow, 1964 (in Russian).
- [23] S.T. Surzhikov, Computational study of the aero-thermodynamics of hypersonic flow around blunted bodies by the example of the analysis of experimental data, *IPMech RAS, Moscow*, 2011 (in Russian).